Applied Soft Computing 48 (2016) 476–490

Contents lists available at ScienceDirect

Applied Soft Computing

journal homepage: www.elsevier.com/locate/asoc

Adaptive B-spline-based fuzzy sliding-mode control for an auto-warehousing crane system

Kuo-Hsiang Cheng

Mechanical and Systems Research Laboratories, Industrial Technology Research Institute, Chutung, Hsinchu 310, Taiwan

ARTICLE INFO

Article history:
Received 2 March 2013
Received in revised form 3 April 2016
Accepted 6 April 2016
Available online 29 July 2016

Keywords:
adaptive control
B-spine
fuzzy control
Lyapunov theorem
sliding mode control

ABSTRACT

In this paper, an adaptive B-splined-based fuzzy sliding mode control (ABFSM) is presented to the application of auto-warehousing crane motion control. The ABFSM comprises an adaptive fuzzy identification controller (AFIC) and a B-spline-based compensation controller (BCC). The AFIC is designed to **approximate the ideal controller of a crane system**. To alleviate the **load of fuzzy rule base construction, only the information from the sliding surface is used as the input of AFIC** such that the conciseness and translucency of the control system can be upgraded. On the other hand, the BCC aims to compensate the approximation error of the AFIC. With the introduction of the B-spline function, the boundary of the approximation error can be represented **by means of** polynomial mapping. Thus, the design of the compensation controller can be **achieved** based on the characteristics of the B-spline function. In this paper, the objective of the ABFSM is to track the distance-speed reference trajectory of the **crane control system**. With the tuning law of the AFIC and the BCC, the stability can also be guaranteed by means of Lyapunov function. To validate the performance of the proposed approach, the ABFSM is applied to auto-warehousing crane motion control under various conditions for x, y, and z directions, respectively. **From the simulation the advantages of the proposed ABFSM are demonstrated, where the capability to handle the uncertainty with efficiency is verified.**

1. Introduction

Owing to its capability to transform engineering experience into applicable control strategy, extensive real-world applications of fuzzy logic have been witnessed [1,2,9,14,17,20,23,25,28]. The key element of fuzzy logic control is that the dynamics of the ill-defined controlled system can be approximated to a certain level by fuzzy reasoning. **Based on the linguistic "IF A THEN B" description, the semantic rule reasoning demonstrates a superior ability than that of the conventional control theory when inaccurate mathematical modeling is encountered.** The characteristics of soft-computation also provide the robustness to operate within a wide range of conditions **when the internal imperfection and external disturbances are considered in the applications.** For industrial approaches, fuzzy controller design is usually performed through empirical experience to define the rule base [1,12]. To attain system automation, the extensions of fuzzy controllers by introducing other techniques have aroused much interest and became the emerging topics in the field of control engineering [4,5,10,22,24,26,27,29,32,33,34].

With the advantages of great capacity, high efficiency, computerized operation, and real-time inventory, auto-warehousing crane system is widely used in industrial applications for storing and accessing heavy cargoes [3,8,12]. The auto-warehousing crane system can move in *x*, *y*, *z* directions, where the positioning accuracy has been challenging since the system is required to operate under different working conditions such as moving distance and weight of load. **Moreover, the estimation of the exact friction model along each direction is also important in order to achieve accurate positioning.** Therefore, identifying real-world auto-warehousing system is a complex task and extracting the knowledge from the real-world applications is laborious and time-consuming.

To achieve control robustness, sliding mode control has been suggested to be good approach for its advantages of uncertainty accommodation and real-time implementation [6,16,18,22,31,35]. However, the unfavorable chattering phenomenon is also introduced by the conventional sliding mode control approaches. To mitigate the adverse phenomenon, the saturation function was proposed but the stability cannot be guaranteed. An approximation error bound estimation mechanism was proposed so that the chattering phenomenon of the control effort can be improved

E-mail address: KHCheng670714@gmail.com

http://dx.doi.org/10.1016/j.asoc.2016.04.002
1568-4946/

Table 1
Specifications for motion control of crane in *x*, *y*, and *z* directions.

Axis	Acceleration (m/s^2)	Deceleration (m/s^2)	Maximum Speed (m/s)	Creep Speed (m/s)	Force Limitation (Newton)	Positioning Accuracy (m)
X	0.5	0.5	3	0.1	−8500 to 8500	less than 0.005
Y	0.2	0.2	2/3	0.1	0–50500	less than 0.005
Z	0.5	0.5	0.5	0.1	−1500 to 1500	less than 0.002

[10,13–15,30]. However, the adaptive law for estimating the error bound makes the bound approach infinity if the main controller is ill-designed. **Regarding the adaptive control approaches with the robust control compensation technique [13,29], the performance is subject to the predetermined attenuation level. If an inappropriate attenuation level is given, the control effort may lead to undesirable large which is difficult to implement.**

The study of B-spline functions has been an emerging topic in engineering field due to its simplicity in implementation [7,11,19]. Based on the manipulation of the control points, the B-spline function can be defined and programmed in a recurrent way, and the input space can be partitioned into sub-domains with B-spline basis functions. **With the advantage of piecewise polynomial mapping, the B-spline-based approaches were applied as an alternative design of fuzzy control systems or artificial neural networks, where the B-spline functions are used as the membership functions or hidden nodes. By incorporating with other learning algorithms, the B-spline-based concept can be used as a powerful tool for curve-fitting, system identification, and control problems [7,19].**

In this paper, an adaptive B-splined-based fuzzy sliding mode control (ABFSM) is presented for auto-warehousing crane motion control**. The proposed approach aims to free the burden of model-based design by introducing fuzzy-logic-based control and a novel control compensater.** The proposed ABFSM comprises an adaptive fuzzy identification controller (AFIC) and a B-spline-based compensation controller (BCC). The AFIC is exploited to approximate the ideal controller for the crane system. **To alleviate the requirement of fuzzy rule construction, in this paper, only the information from the sliding surface is exploited as the input signal of AFIC such that the conciseness and translucency of the control system can be upgraded.** On the other hand, to avoid the shortcoming of the chattering of the sliding mode control, the BCC is exploited to compensate the approximation error of the AFIC. **With the introduction of the B-spline function, the boundary of approximation error can be represented by means of polynomial mapping. The proposed BCC provides a moderate way to compensate the performance of the AFIC when the boundary of approximation error is unavailable in advance.** Moreover, with the adoption of B-spline concept, the function of the compensation controller can be easily undertaken by a microprocessor, **where the function can be defined in a recurrent way based on the given knot vector. Thus, the design of the compensation controller can be easily implemented.** In this paper, with the tuning law of the AFIC and the BCC, the objective of the ABFSM is to track the distance-speed reference trajectory of the warehousing crane system while the stability of closed-loop control system can also be guaranteed by the means of Lyapunov function. To validate the performance of the proposed approach, the ABFSM is applied to the auto-warehousing crane motion control under various loading conditions in *x*, *y*, and *z* direction, respectively. Simulation is conducted to demonstrate the advantages of the proposed ABFSM, where the capability to handle the uncertainty with efficiency is verified. This paper is organized as follows. In section 2, the dynamics of the auto-warehousing crane system and the design of distance-speed reference curve are given. In section 3, the designs of the AFIC and BCC are given. In section 4, the design of the ABFSM and the stability analysis are represented. In section 5, to investigate the capabilities of the proposed approach, the ABFSM is applied to the crane system control with different working conditions. Finally, the conclusion is given in section 6.

Table 2
Parameters of reference curve.

Axis	Minimum $S_{max\text{-}speed}$ (m)	Deceleration (m)	Maximum Speed (m/s)	
x	0.3	0.2	0.013	
y	0.2	0.2	upward 0.002	downward 0.005
z	0.2	0.2	0.002	

Table 3
Parameters for the crane motion equations in *x*, *y*, and *z* directions.

Axis		x	y	z
Crane mass	loaded	1.5×10^4 kg	5×10^3 kg	2×10^3 kg
	unloaded	1.35×10^4 kg	3.5×10^3 kg	5×10^2 kg
Friction Coefficient	α_s	0.03	none	0.03
	α_d	0.001	none	0.001
Time constant τ_k		0.1 s	0.07 s	0.05 s
Braking constant $C_{brake,k}$		5×10^5	3.5×10^5	2×10^5

2. Design of the auto-warehousing crane system

2.1. Motion equations of the crane system

In this subsection, the dynamics of the auto-warehousing crane system of the *x*, *y* and *z* directions, and the specifications are given in Tables 1–3, are discussed [12]. The motion equations of the crane system of the *x*, *y*, and *z* directions are described below.

1) For the *x* and *z* directions, the motion equations are given as follows:

$$m_k \ddot{S}_k(t) = F_{input,k}(t) - \alpha_k N_k \tag{1}$$

$$m_k \ddot{S}_k(t) = F_{brake,k} \tag{2}$$

where $k = x$ and z. The parameter m_k is the mass of crane, $S_k(t)$is the distance of crane to the start position at time t, $F_{input,k}(t)$ is the control input to the crane system with the consideration of delay of mechanical transmission, α_k is the coefficient of friction, which can be given with the coefficient of static friction $a_{s,k}$ when $\dot{S}_k(t) = 0$ or with the coefficient of dynamic friction $a_{d,k}$ when $\dot{S}_k(t) > 0$. $N_k = gm_k = 9.81m_k$ is the normal force. $F_{brake,k}$is the braking force when the brake is activated. In this paper, the time delay of mechanical transmission is assumed as a time constant and the control inputs are regulated as

$$F_{input,k}(t) = \left[F_{input,k}(t-1) - u_k(t)\right] \exp\left(\frac{-T_k}{\tau_k}\right) + u_k(t) \tag{3}$$

where $T_k = 0.025$ s is the sampling time, τ_k is the time constant of delay, and $u_k(t)$ is the control input of the controller. In (3), the

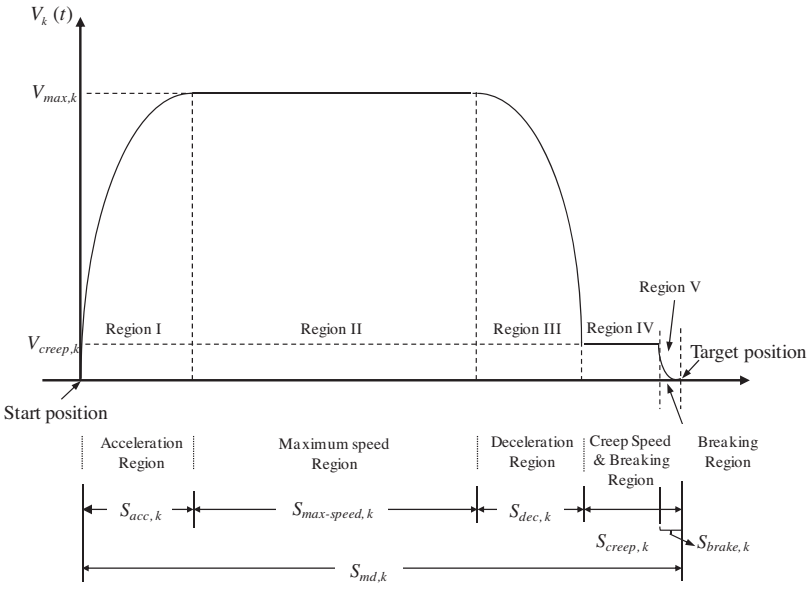

Fig. 1. Distance–speed reference curve for k direction ($k = x$, y and z).

braking force can be regarded as a resisting force that decreases exponentially with speed, which is expressed as

$$F_{brake,k} = -C_{brake,k}\left(\frac{dS_k(t)}{dt}\right)^{1.5} \tag{4}$$

where $C_{brake,k}$ is the constant of braking force for the k direction.

2) For the y direction, **the motion equations can be divided into the upward motion and the downward motion, which are given as follows:**

$$m_y\ddot{S}_y(t) = \begin{cases} F_{input,y}(t) - m_y g - F_{friction}, & \text{when } F_{input,y}(t) > m_y g + F_{friction} \quad \text{(upward motion)} \\ F_{input,y}(t) - m_y g + (F_{friction}), & \text{when } F_{input,y}(t) > 0.94 m_y \quad \text{(downward motion)} \\ F_{brake,y} - m_y g, & \text{otherwise} \end{cases} \tag{5}$$

$$F_{input,y}(t) = \left[F_{input,y}(t-1) - F_{accumulated}(t)\right]\exp\left(\frac{-T_s}{\tau_y}\right) + F_{accumulated}(t) \tag{6}$$

$$F_{accumulated,y}(t) = F_{accumulated,y}(t-1) + u_y(t) \tag{7}$$

where m_y is the mass of crane in the y direction and $F_{friction}$ is the friction force, which is considered as a constant of 50 N. In y-directional motion control, the controller takes over from the brake system when the input force to the crane overcomes the gravity and friction force for upward motion. For downward motion, it takes over when the input force is larger than $0.94m_y$ to prevent the crane from falling due to gravity. Otherwise, the brake is always applied on the crane to keep it motionless. The braking force in the y direction is expressed as follow

$$F_{brake,y} = \begin{cases} m_y g\delta(\dot{S}_y(t)) - C_{brake,y}\dot{S}_y^{1.5}(t) \text{(upward motion)} \\ m_y g + C_{brake,y}\dot{S}_y^{1.5}(t) \quad \text{(downward motion)} \end{cases} \tag{8}$$

where

$$\delta(\dot{S}_y(t)) = \begin{cases} 1, & \text{when } \dot{S}_y(t) = 0 \\ 0, & \text{otherwise} \end{cases} \tag{9}$$

and $C_{brake,y}$ is the constant of braking force in the y direction. The parameters of the crane system and loading conditions for the x, y, and z directions are listed in Table 2 and 3.

2.2. Design of reference curve

To achieve efficient crane control and accurate positioning, a distance-speed reference curve for each direction is predefined according to the specifications of the crane system such as the maximum speed, acceleration and deceleration. The distance-speed reference curve is designed to control the crane system to undergo the processes of acceleration, maximum speed, deceleration, creep speed, and braking along each direction. The profile of the distance-speed reference curve for each direction is shown in Fig. 1, where the moving distance of the crane $S_{md,k}$ is known in advance and can be written as

$$S_{md,k} = S_{acc,k} + S_{max-speed,k} + S_{dec,k} + S_{creep,k} + S_{brake,k} \tag{10}$$

where $k = x$, y, and z. In (10), the moving distance is divided into five regions, and the length of each region is denoted as $S_{acc,k}$,$S_{max-speed,k}$,$S_{dec,k}$,$S_{creep,k}$, and$S_{brake,k}$, respectively. In Region I, the crane is accelerated from the starting point to a determined maximum speed $V_{max-speed,k}$, which is calculated according to the moving distance in each direction. **However, the determined maximum speed should not exceed the given maximum speed in** Table 2. In Region II, the crane is expected to move at the speed $V_{max-speed,k}$. In Region, III, the region is designed to decelerate the crane from $V_{max-speed,k}$ to the creep speed $V_{creep,k}$. **In Region IV, the crane is expected to move at the speed of $V_{creep,k}$ before it reaches Region V.** In Region V, the brake system takes over the control to stop the crane. **For the simplicity of the reference trajectory design, $S_{creep,k}$ and $S_{brake,k}$ are defined with fixed values as depicted in** Table 1 **and** the lengths of $S_{acc,k}$,$S_{max-speed,k}$,$S_{dec,k}$ vary according to the desired moving distance in the k direction.

To determine the distances of Region I, II, and III, first, Newton's motion law is applied to the motions of Region I and III, which are given as follows:

$$V_{max-speed,k}^2 = 2a_{acc,k}S_{acc,k} \tag{12}$$

$$V_{max-speed,k}^2 = V_{creep,k}^2 + 2a_{dec,k}S_{dec,k} \tag{13}$$

Since that the acceleration and deceleration in each direction are given with the same values, it can be rewritten as follows.

$$S_{dec,k} = \frac{1}{2a_k}(2a_k S_{acc,k} - V_{creep,k}^2) = S_{acc,k} - \frac{1}{2a_k}V_{creep,k}^2 \tag{14}$$

where $a_k = a_{acc,k} = a_{dec,k}$. Based on (14), (10) can be shown as follows

$$S_{acc,k} = 0.5\left(S_{md,k} - (S_{max-speed,k} + S_{creep,k} + S_{break,k}) + \frac{1}{2a_k}V_{creep,k}^2\right) \quad (15)$$

With (12) and (15), it can be found that if $S_{max-speed,k}$ is given with the minimum value as given in Table 2, then $S_{acc,k}$ and $V_{max-speed,k}$ will be maximized. Therefore, to determine the value of $S_{acc,k}$, the minimum value of $S_{max-speed,k}$ is first used in (15) to calculate the maximum value of $V_{max-speed,k}$. If the obtained $V_{max-speed,k}$ is less than the maximum value in Table 1, it will be considered as an applicable condition, or $V_{max-speed,k}$ will be determined according to the maximum value. With $V_{max-speed,k}$ is defined, then the finalized $S_{acc,k}$ and $S_{dec,k}$ will be given by (14) and (15).

3. Design of ABFSM

3.1. Sliding mode fuzzy inference control system

Sliding mode control has been a wildly discussed control technique due to its capability to handle internal variation and external disturbance of the controlled system. In order to elaborate the design of ABFSM, a tracking error is derived from the difference between the state trajectory x and the desired command x^c, which is given as follows.

$$e = x^c - x. \quad (16)$$

With a sliding surface is defined as

$$s_f = \dot{e} + \beta_1 e + \beta_2 \int_0^t e \; d\tau \quad (17)$$

Where β_1 and β_2 are positive constants. Based on (17), the objective of proposed ABFSM is to force the system state trajectory toward to the sliding surface and stay on it, i.e., $s_f(t) = \dot{s}_f(t) = 0$. Thus, the equivalent dynamics of the controlled system is governed by

$$\ddot{e} + \beta_1 \dot{e} + \beta_2 e = 0 \quad (18)$$

With (18), it implies that $\lim_{t\to\infty} e(t) = 0$ for any starting initial conditions, i.e., the tracking of the reference trajectory is asymptotically

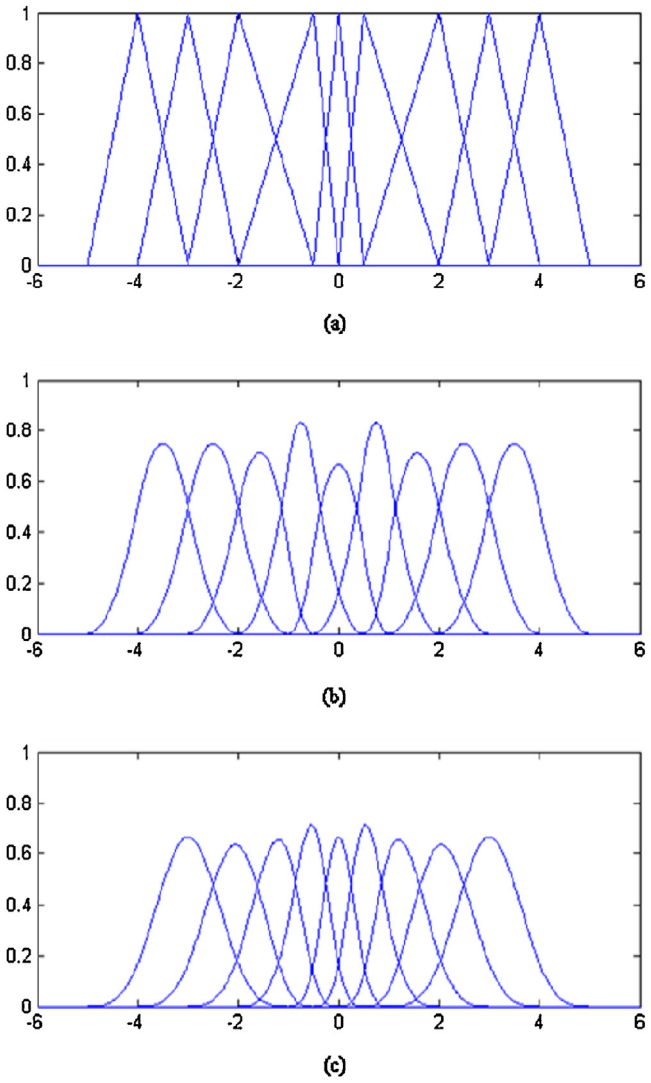

Fig. 2. The B-spline basis functions.

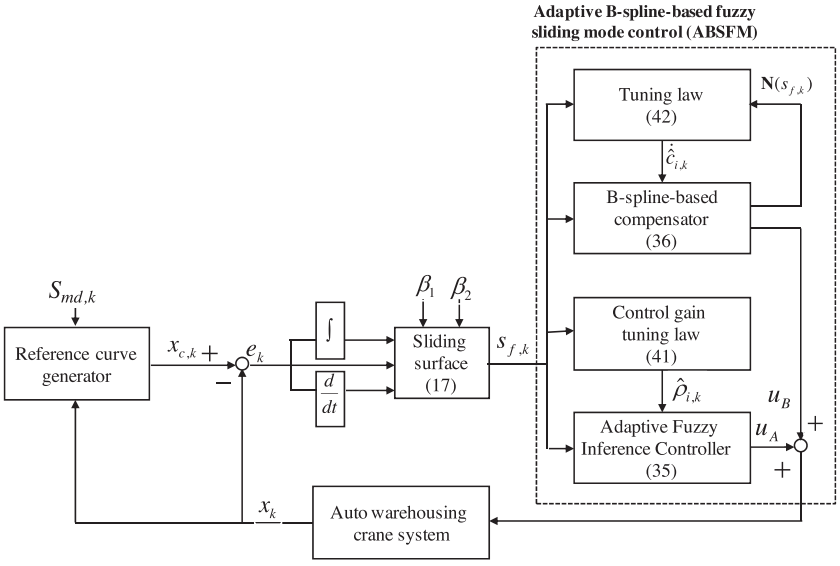

Fig. 3. The diagram of the proposed ABFSM crane motion control for k direction ($k = x$, y, and z).

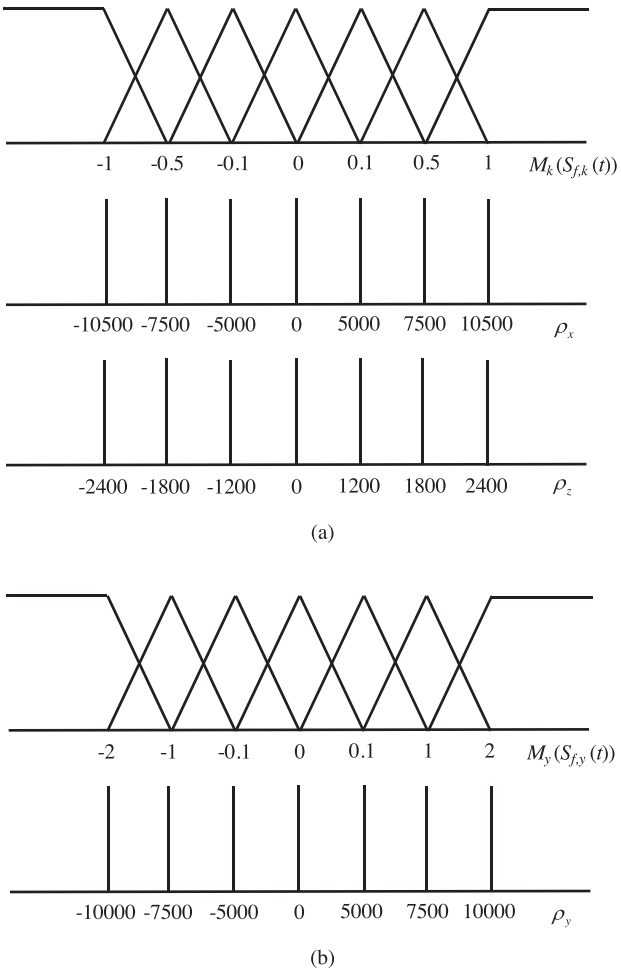

Fig. 4. (a) Premise and consequence parameters of the AFIC for *x* and *z* direction (b) Premise and consequence parameters of the AFIC for *y* direction.

achieved if the gains $\beta_1$and β_2 are selected properly [10]. In the traditional fuzzy system design, the controlled system dynamics is often used to form the input space of the control system. Assume there are *n* inputs, the fuzzy sets associate to the *i*-th input will be defined in the corresponding dimension. However, when the number of dimension increases, the number of the generated fuzzy rules grows exponentially. To overcome the problem of "curse of dimensionality" and upgrade the conciseness of fuzzy rule base, in this paper, a fuzzy-logic-system using information from sliding surface as its input is defined in order to alleviate the burden of fuzzy rules constitution. The fuzzy rules are given in the following form:

$$\text{Rule } \ i: \ \text{IF } s_{f,k} \text{ is } M_{i,k}(s_{f,k}(t)) \quad \text{THEN} \quad u_k(t) = \rho_{i,k} \tag{19}$$

where $\rho_{i,k}$ and $M_{i,k}$ the *i*-th control gain and the label of fuzzy set of the *k* direction, respectively.

In the AFIC, the triangular membership functions and singletons are used to define the IF-part and THEN-part inference. Thus, the output of the AFIC can be defined based on the center-of-gravity defuzzification method.

$$u_k(t) = \frac{\sum_{i=1}^{m} w_i \rho_{i,i}}{\sum_{i=1}^{m} w_i} = \boldsymbol{\rho}^T \mathbf{w} \tag{20}$$

where *m* is the number of rules, w_i is the firing strength of the *i*-th rule.

Table 4
Spent time, final position, and positioning accuracy (3 m and 30 m, *x* direction).

Axis	x	
Distance (m)	3	30
Loading condition	loaded	unloaded
Crane mass (kg)	1.5×10^4	1.35×10^4
Spent time (s)	7.125	18.675
Final position (m)	3.0001	29.9981
Position accuracy (m)	0.0001	0.0019

Table 5
Spent time, final position, and positioning accuracy (3 m and 20 m, *y* direction).

Axis	y			
Distance (m)/Direction	3/up	20/up	3/down	20/down
Loading condition	loaded	unloaded	loaded	Unloaded
Crane mass (kg)	5×10^3	3.5×10^3	5×10^3	3.5×10^3
Spent time (s)	8.8	34.675	9	35
Final position (m)	2.9997	19.9995	3.0018	19.9985
Position accuracy (m)	0.0003	0.0005	0.0018	0.0015

Table 6
Spent time, final position, and positioning accuracy (2 m, *z* direction).

Axis	z	
Distance (m)	2	2
Loading condition	loaded	unloaded
Crane mass (kg)	2×10^3	5×10^2
Spent time (s)	6.1	5.70
Final position (m)	2.0015	1.9988
Position accuracy (m)	0.0015	0.0012

3.2. Design of B-spline function

To describe the operation of the B-spline compensator, the B-spline basis functions is reviewed first. Define the knot vector **T,** which comprises a set of knots from a sequence of real numbers [7,19].

$$\mathbf{T} = \mu_0 \mu_1 \ldots \mu_{2p+j}. \tag{21}$$

In (21), *p* is the parameter to determine the number of B-spline basis functions and *j* denotes the order. Thus, the *i*-th B-spline basis function of order *j* denotes$N_{i,j}(\mu)$, can be defined as follows:

$$N_{i,j}(\mu) = \frac{(\mu - \mu_i) N_{i,j-1}(\mu)}{\mu_{i+j-1} - \mu_i} + \frac{(\mu_{i+j} - \mu) N_{i+1,j-1}(\mu)}{\mu_{i+j} - \mu_{i+1}}, \ \mu_i \le \mu < \mu_{i+j}, \tag{22}$$

$$N_{i,1}(\mu) = \begin{matrix} 1 & \text{if} \ \ \mu_i \le \mu < \mu_{i+j} \\ 0 & \text{otherwise} \end{matrix}. \tag{23}$$

The function of (22) is a recursive definition which speficies how the *j*-th order function is constructed from two blending functions of order *j*-1. The B-spline basis functions with $p = 4$ and different order 2, 3, and 4 are given in Fig. 2(a–c), respectively. With different orders and knot vectors, different B-spline basis functions are represented. **To describe the polynomial mapping of the B-spline functions, assume a coefficient set** $\mathbf{C} = \begin{bmatrix} c_0 & c_1 & \cdots & c_p & \cdots & c_{2p-1} & c_{2p} \end{bmatrix}^T$ **with 2*p*+1 elements is given, then the B-spline function** $f_b(\mu)$ **can be defined as follows.**

$$f_b(\mu) = \sum_{i=0}^{2p} c_i N_{i,j}(\mu) = \mathbf{C}^T \mathbf{N}(\mu), \tag{24}$$

where $\mathbf{N}(\mu) = \begin{bmatrix} N_{0,j}(\mu) & N_{1,j}(\mu) & \cdots & N_{2p,j}(\mu) \end{bmatrix}^T$. In this B-spline compensation controller, the property of partition of unity is exploited, where the output of each B-spline basis function is positive and the summation of all B-spline basis function outputs is equal to 1. In this paper, the function of (24) is used to describe

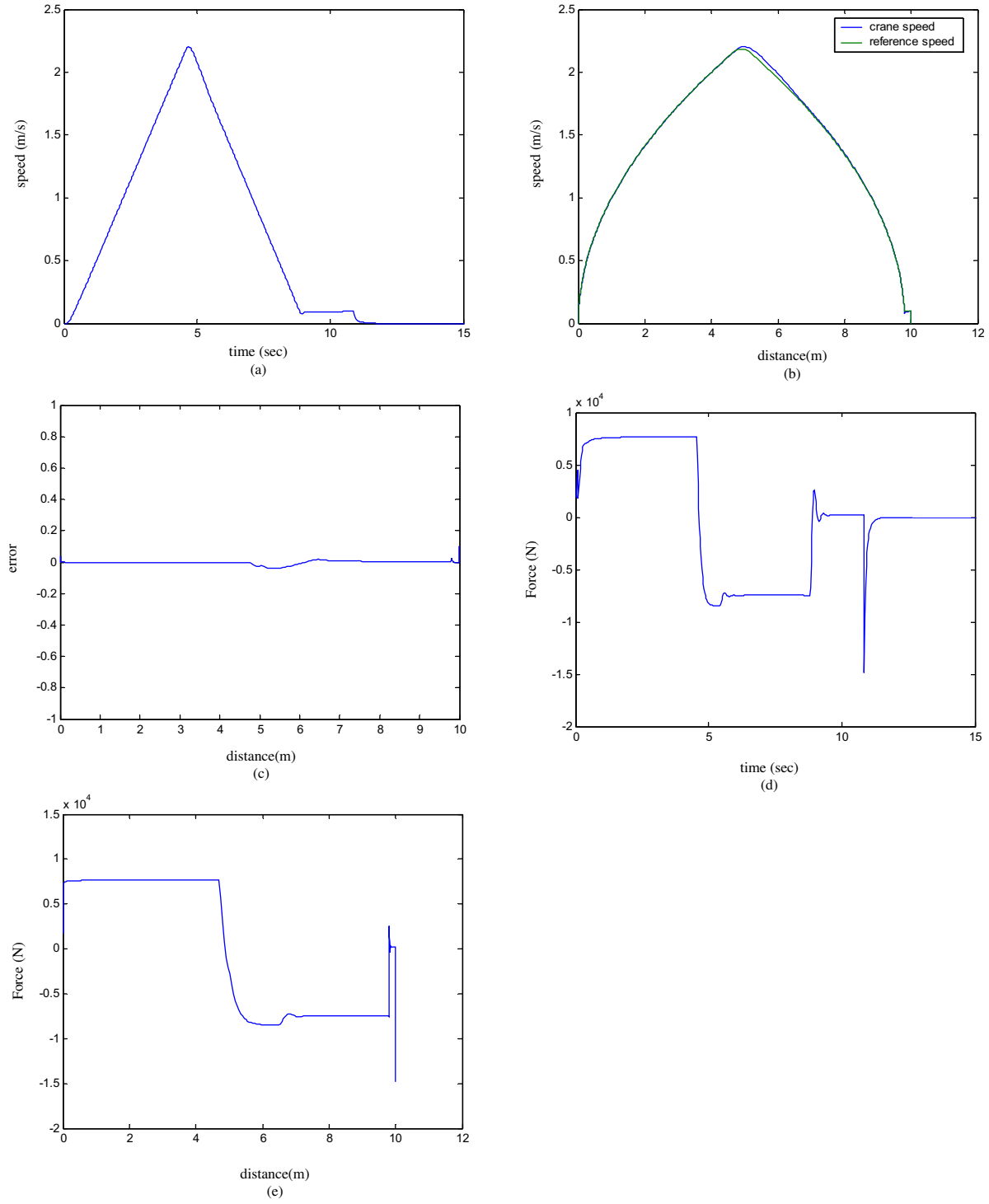

Fig. 5. *X*-directional distance–speed control of the crane system (10 m, loaded). (a) Time–speed curve. (b) Distance–speed curve. (c) Error between crane speed and reference. (d) Time–force curve. (e) Distance–force curve.

the approximation error. **Since the bound of the lumped approximate error cannot be exactly obtained in advance, the elements of C are difficult to obtain. To overcome this shortcoming, the adaptive parameter estimation based on the Lyapunov theorem is exploited to ensure the performance of BCC.**

3.3. Design of ABFSM

The control diagram of the proposed ABFSM is described in Fig. 3, where the output can be given as follows

$$u_{ABFSM} = u_A + u_B, \tag{25}$$

where u_A is the output of the AFIC and u_B is the output of the B-spline-based compensator. Based on (1), (3) and (5)–(7), the controlled system can be given as follows.

$$\ddot{x}_k(t) = f_k + u_k(t) \tag{26}$$

where $x_k(t) = S_k(t)$, the controlled system dynamics of the k direction can be defined as

$$f_k = \frac{1}{m_k}\left[F_{input,k}(t-1) - u_k(t)\right] \exp\left(\frac{-T_k}{\tau_k}\right) - \alpha_k N_k \tag{27}$$

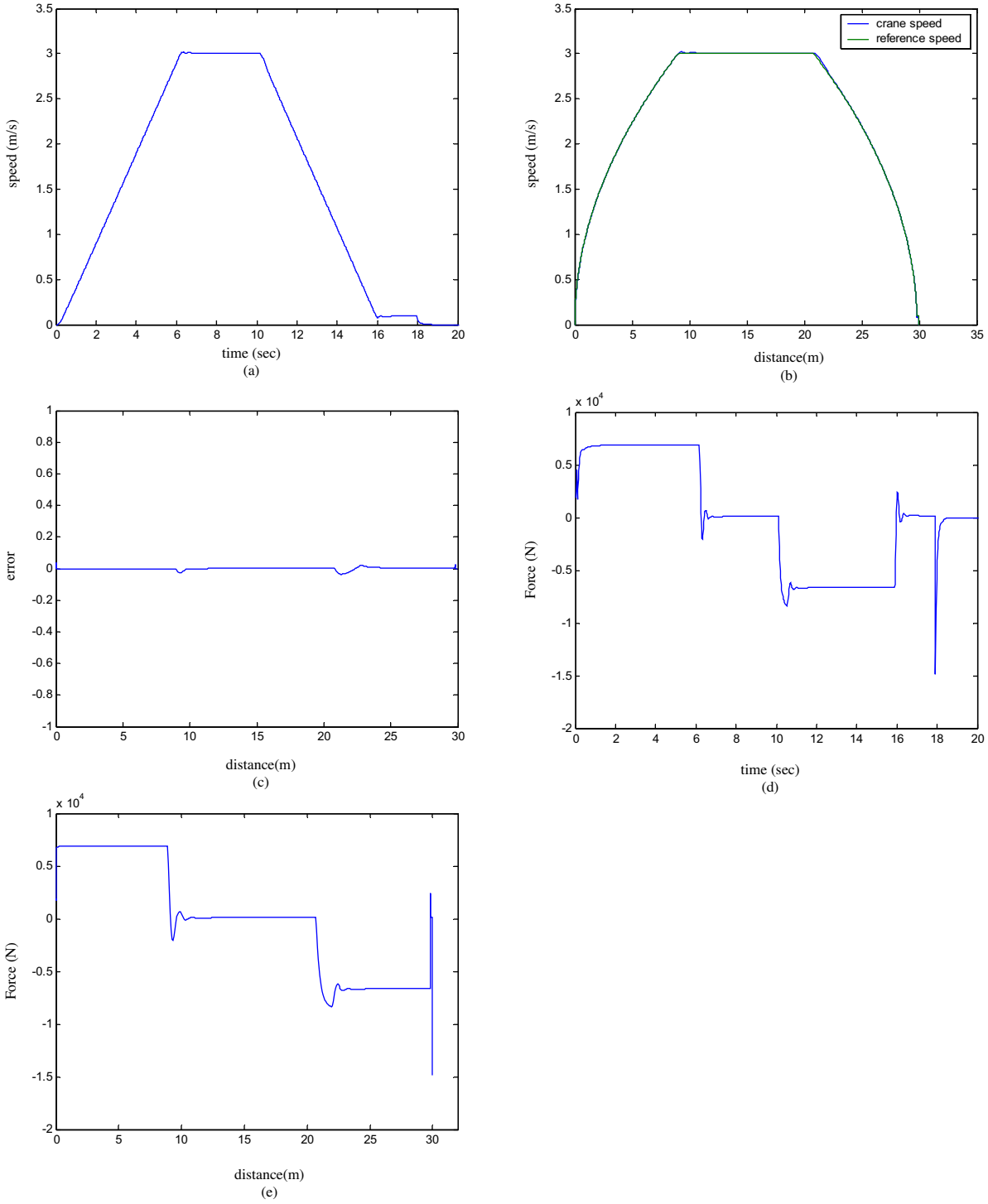

Fig. 6. *X*-directional distance–speed control of the crane system (30 m, unloaded). (a) Time–speed curve. (b) Distance–speed curve. (c) Error between crane speed and reference. (d) Time–force curve. (e) Distance–force curve.

for $k = x$ and z, and

$$f_y = \frac{1}{m_y}\left[F_{input,y}(t-1) - F_{accumulated}(t)\right]\exp\left(\frac{-T_s}{\tau_y}\right)F_{accumulated,y}(t-1) - m_y g - F_{friction}\,(\text{upward motion}) \tag{28}$$

$$f_y = \frac{1}{m_y}\left[F_{input,y}(t-1) - F_{accumulated}(t)\right]\exp\left(\frac{-T_s}{\tau_y}\right)F_{accumulated,y}(t-1) - m_y g + F_{friction}\,(\text{downward motion}) \tag{29}$$

For the real-world crane system, the dynamics of unloaded condition are well known according to the specifications or measurement. Thus, the unloaded model of the crane system can be rewritten.

$$\ddot{x}_k(t) = f_k^u + u_k(t), \tag{30}$$

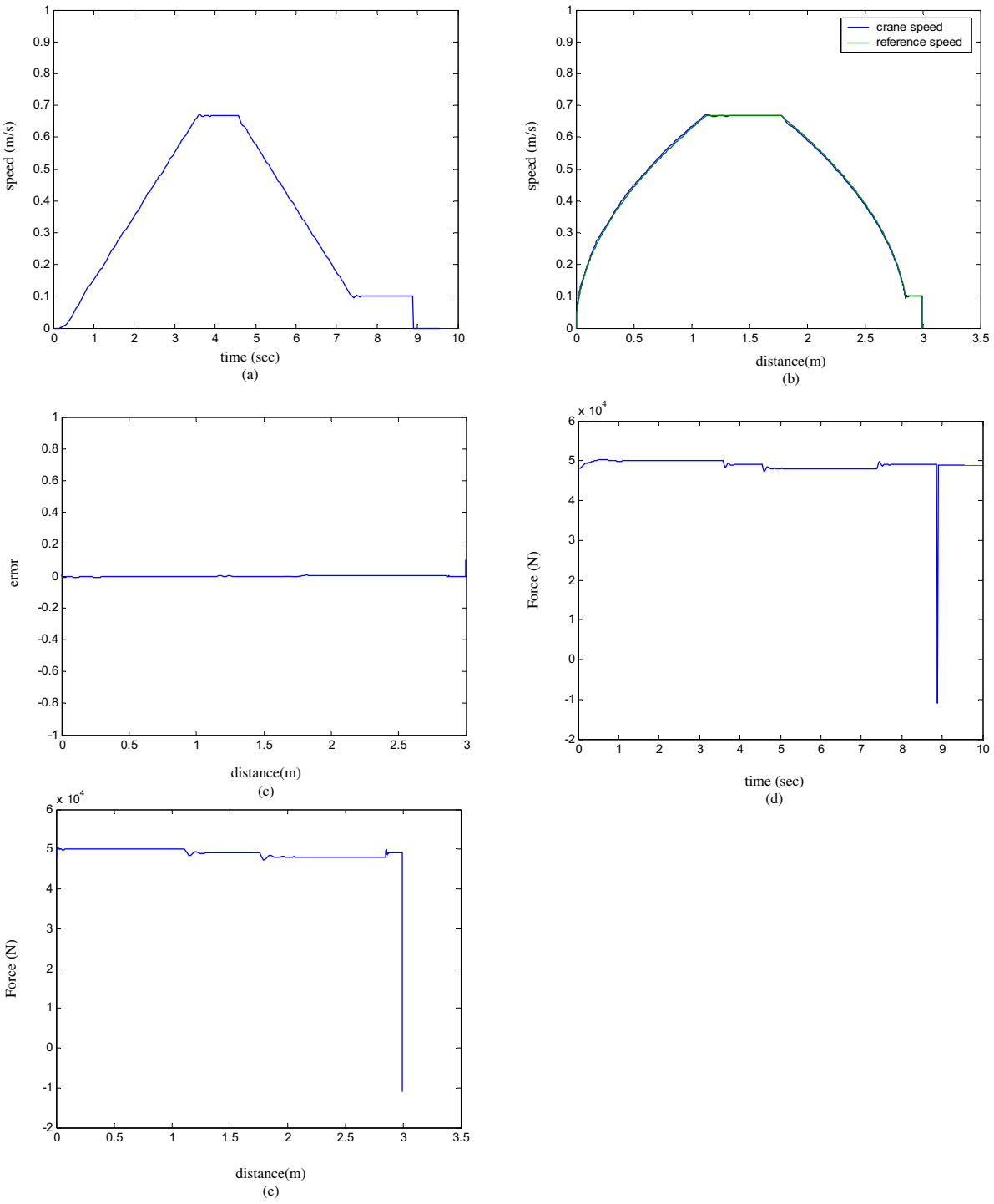

Fig. 7. *Y*-directional upward distance–speed control of the crane system (3 m, loaded). (a) Time–speed curve. (b) Distance–speed curve. (c) Error between crane speed and reference. (d) Time–force curve. (e) Distance–force curve.

where f_k^u represents the unloaded behavior of the crane system. However, for the loaded conditions, the dynamics of the crane system deviate from the unloaded case. Thus, the controlled system can be modified as

$$\ddot{x}_k(t) = f_k^l + u_k(t) = f_k^u + \Delta f + u_k(t). \tag{31}$$

In (31), Δf denotes the lumped term of dynamics variation and the uncertainty due to different loading conditions, whcih can be assumed to be bounded, i.e., $|\Delta f| \le D$. The parameter D can be given with a positive constant. Substituting (25) into (31) and based on (16) and (17), it yields

$$\dot{s}_{f,k} = \ddot{e}_k + k_1\dot{e}_k + k_2 e_k = u_k^* - u_{AFIC} - u_B. \tag{32}$$

where $u_k^* = -f_k^u + \ddot{x}_k^c - \beta_1\dot{e}_k - \beta_2 e_k$ for the unloaded condition and $u_k^* = -f_k^l + \ddot{x}_k^c - \beta_1\dot{e}_k - \beta_2 e_k$ for the loaded conditions. According to the approximation ability, there exists an optimal fuzzy system $u_{A,k}^*$ to approximate u_k^* [10].

$$u_{A,k}^* = \boldsymbol{\rho}_k^{*T}\mathbf{w}_k \tag{33}$$

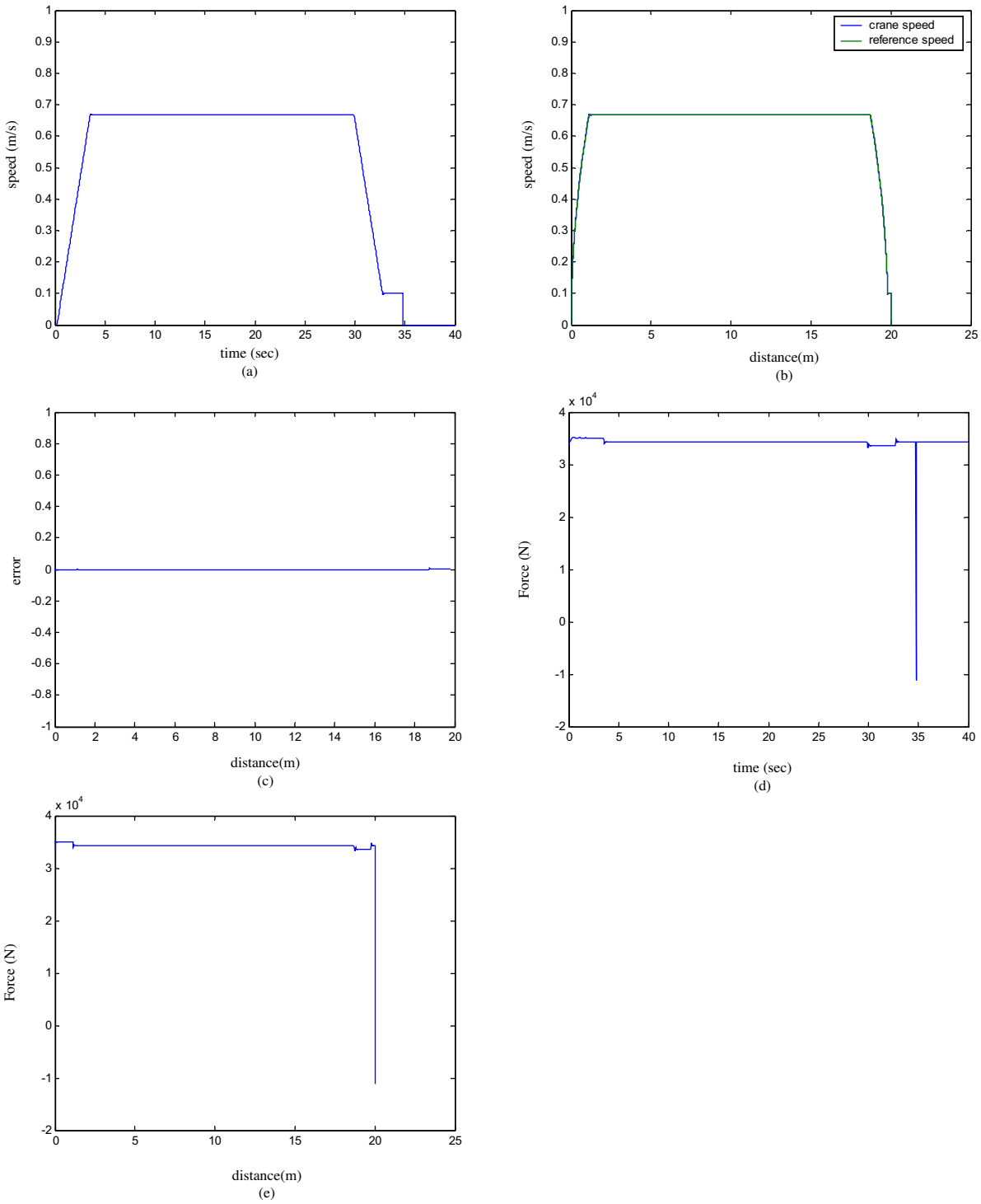

Fig. 8. *Y*-directional upward distance–speed control of the crane system (20 m, unloaded). (a) Time–speed curve. (b) Distance–speed curve. (c) Error between crane speed and reference. (d) Time–force curve. (e) Distance–force curve.

and the "approximation error" is defined as

$$\varepsilon_k = u_k^* - u_{A,k}^* \quad (34)$$

In (34), the approximation error is assumed to be bounded by a constant E_k ($|\varepsilon_k| \le E_k$). In fact, the optimal parameter vectors in (20) to approximate the ideal controllers of the three directions are difficult to determine. Thus, an estimate function of (20) is defined as

$$\hat{u}_{A,k} = \hat{\rho} k T \mathbf{w}_k \quad (35)$$

where $\hat{\rho}_k$ is the estimation of $\boldsymbol{\rho}_k^*$ for the x, y, and z directions, respectively.

3.4. Stability analysis with the B-spline-based compensator

To compensate the approximation error, the output of the B-spline-based compensation controller is given according to (24).

$$u_{B,k} = f_b(s_{f,k}(t)) = sgn(s_{f,k}(t)) \sum_{i=0}^{2p} c_{i,k} N_{i,k}(s_{f,k}(t)), \quad (36)$$

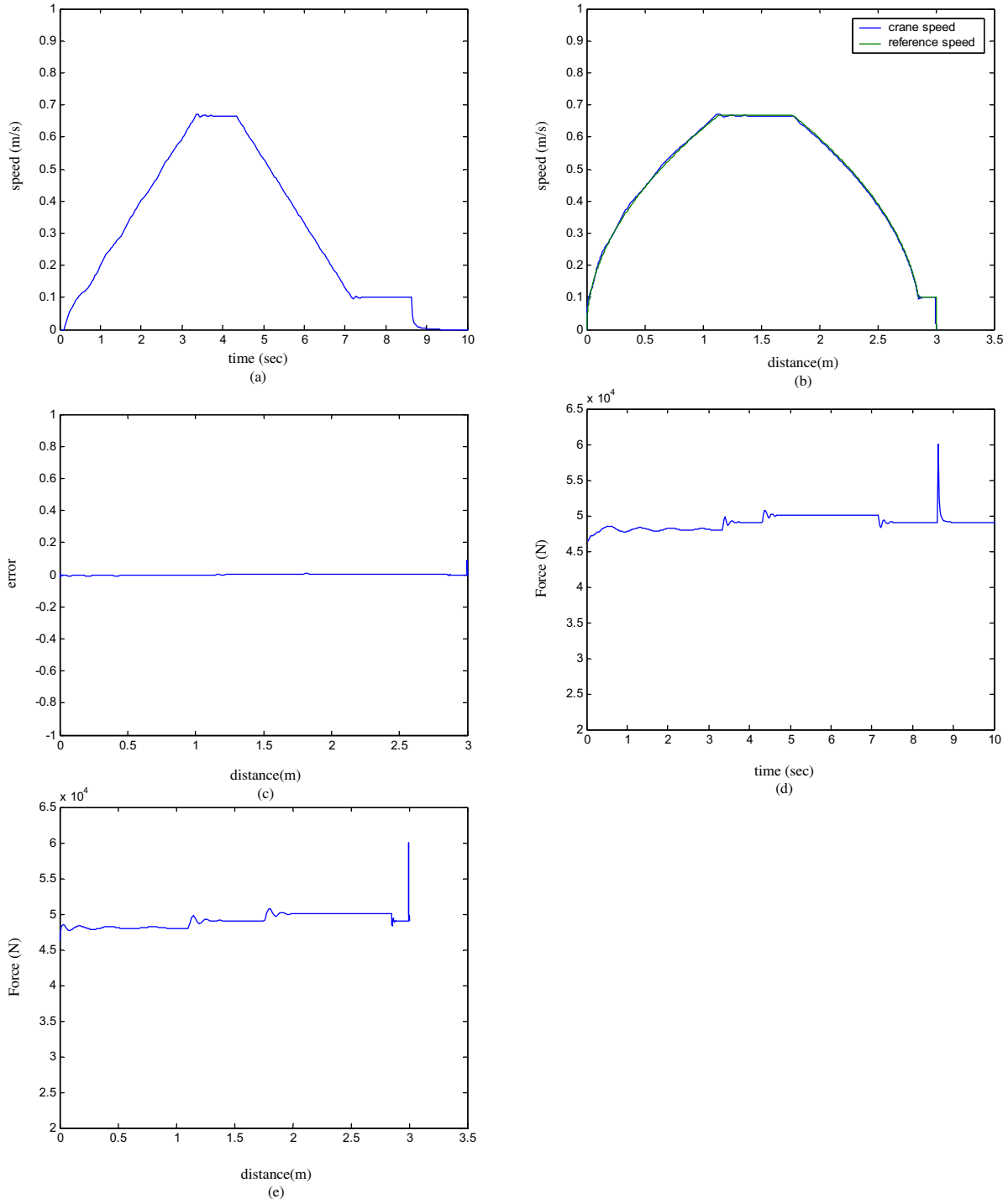

Fig. 9. *Y*-directional downward distance–speed control of the crane system (3 m, loaded). (a) Time–speed curve. (b) Distance–speed curve. (d) Time–force curve. (e) Distance–force curve.

To alleviate the compensation controller design, suppose that there exists an ideal set of control point as following.

$$0 \le |\varepsilon_k| \le \sum_{i=0}^{2p} c_{i,k}^{*} N_{i,k}(s_{f,k}(t)), \tag{37}$$

Thus, (28) can be rewritten

$$u_{B,k} = sgn(s_{f,k}(t)) \sum_{i=0}^{2p} \hat{c}_{i,k} N_{i,k}(s_{f,k}(t)), \tag{38}$$

where $\hat{c}_{i,k}$is the i-th element of $\mathbf{C}_k$for the x, y, and z directions, respectively.

To investigate the stability of the ABFSM, define a Lyapunov function candidate in the following form

$$V_k = \frac{1}{2} s_{f,k}^2 + \frac{\tilde{\rho} k T \tilde{\rho}_k}{\eta_\alpha} + \frac{1}{\eta_c} \sum_{i=0}^{2p} \tilde{c}_{i,k}^2, \tag{39}$$

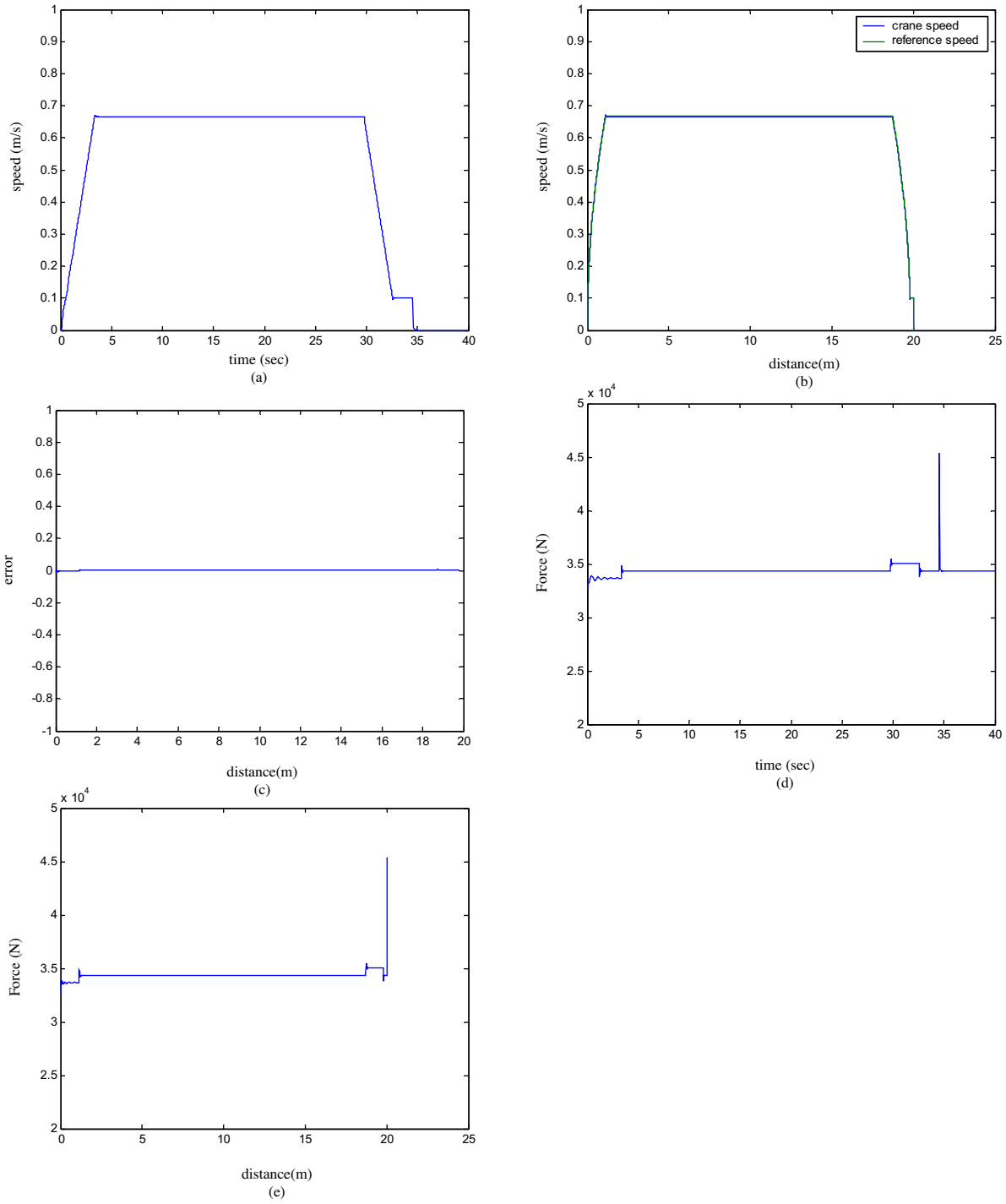

Fig. 10. *Y*-directional downward distance–speed control of the crane system (20 m, unloaded). (a) Time–speed curve. (b) Distance–speed curve. (c) Error between crane speed and reference. (d) Time–force curve. (e) Distance–force curve.

where $k = x, y$ and z, $\tilde{c}_{i,k} = c^*_{i,k} - \hat{c}_{i,k}$, $i = 0, 1, \ldots, 2p$. Differentiating (39) with respect to time and using (35) gives

$$\begin{aligned}\dot{V}_k &= s_{f,k}\dot{s}_{f,k} + \frac{\tilde{\rho}kT\dot{\tilde{\rho}}_k}{\eta_\alpha} + \frac{1}{\eta_c}\sum_{i=0}^{2p}\tilde{c}_{i,k}\dot{\tilde{c}}_{i,k} \\ &= s_{f,k}(\tilde{\rho}kT\boldsymbol{w}_k + \varepsilon_k + u_{B,k}) + \frac{\tilde{\rho}kT\dot{\tilde{\rho}}_k}{\eta_\alpha} + \sum_{i=0}^{2p}\frac{\tilde{c}_{i,k}\dot{\tilde{c}}_{i,k}}{\eta_c} \\ &= \tilde{\rho}kT(s_{f,k}\boldsymbol{w}_k + \frac{\dot{\tilde{\rho}}_k}{\eta_\alpha}) + s_{f,k}(\varepsilon_k + u_{B,k}) + \sum_{i=0}^{2p}\frac{\tilde{c}_{i,k}\dot{\tilde{c}}_{i,ki}}{\eta_c}\end{aligned} \tag{40}$$

where $\tilde{\rho}_k$ is the estimation error of $\boldsymbol{\rho}_k$. To assure the convergence, the learning laws are derived as follows

$$\dot{\tilde{\rho}}_k = -\dot{\hat{\rho}}_k = -s_{f,k}\eta_{\boldsymbol{\alpha}}\boldsymbol{w}_k \tag{41}$$

Then, (40) can be rewritten as

$$\begin{aligned}\dot{V}_k &= s_{f,k}(\varepsilon_k + u_{B,k}) + \sum_{i=0}^{2p}\frac{\tilde{c}_{i,k}\dot{\tilde{c}}_{i,k}}{\eta_c} \\ &= s_{f,k}(\varepsilon_k - sgn(s_{f,k}(t))\sum_{i=0}^{2p}(\hat{c}_{i,k})N_{i,j}(s_{f,k}(t))) + \sum_{i=0}^{2p}\frac{\tilde{c}_{i,k}\dot{\tilde{c}}_{i,k}}{\eta_c}.\end{aligned} \tag{42}$$

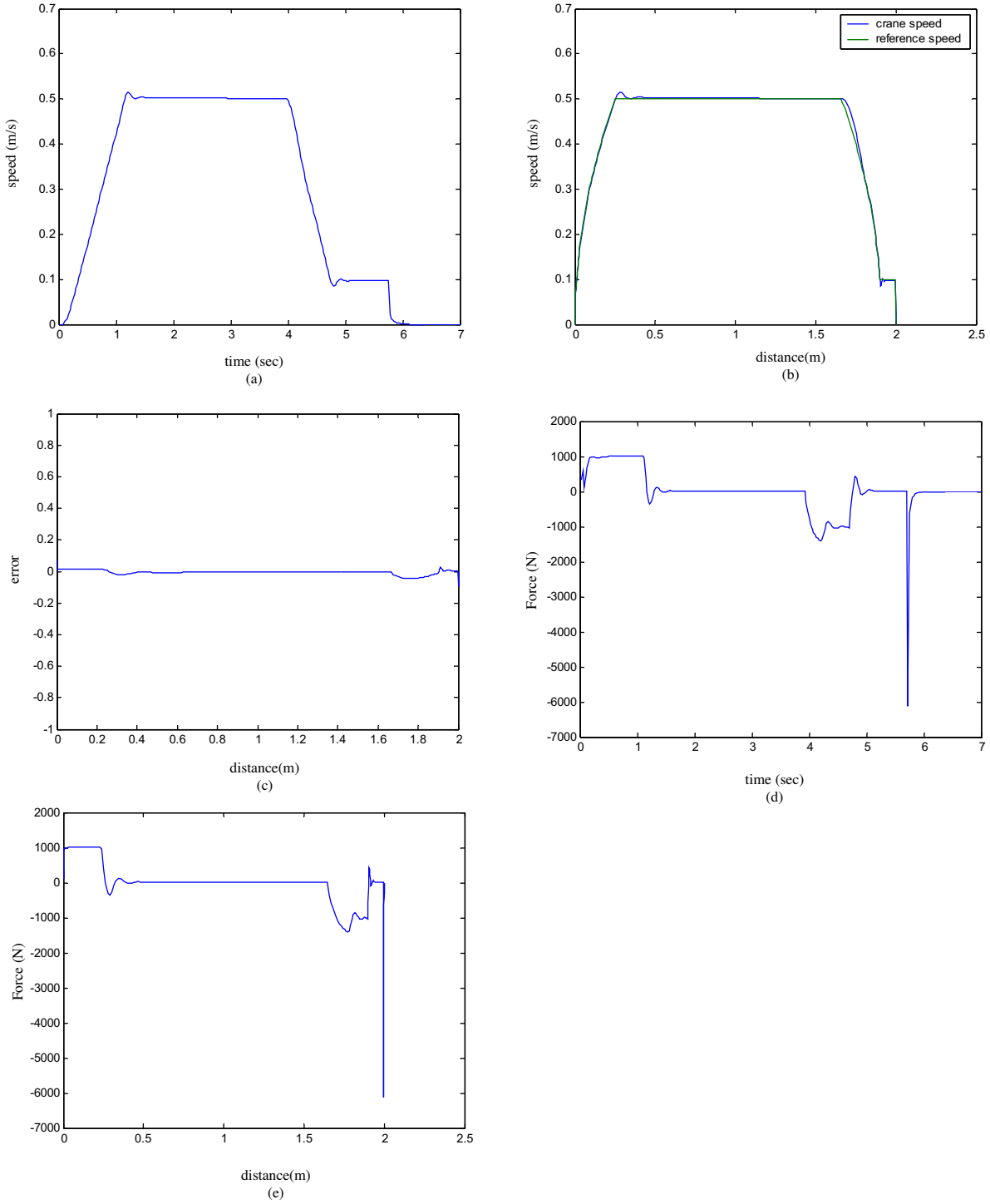

Fig. 11. *Z*-directional distance–speed control of the crane system (2 m, loaded). (a) Time–speed curve. (b) Distance–speed curve. (c) Error between crane speed and reference. (d) Time–force curve. (e) Distance–force curve.

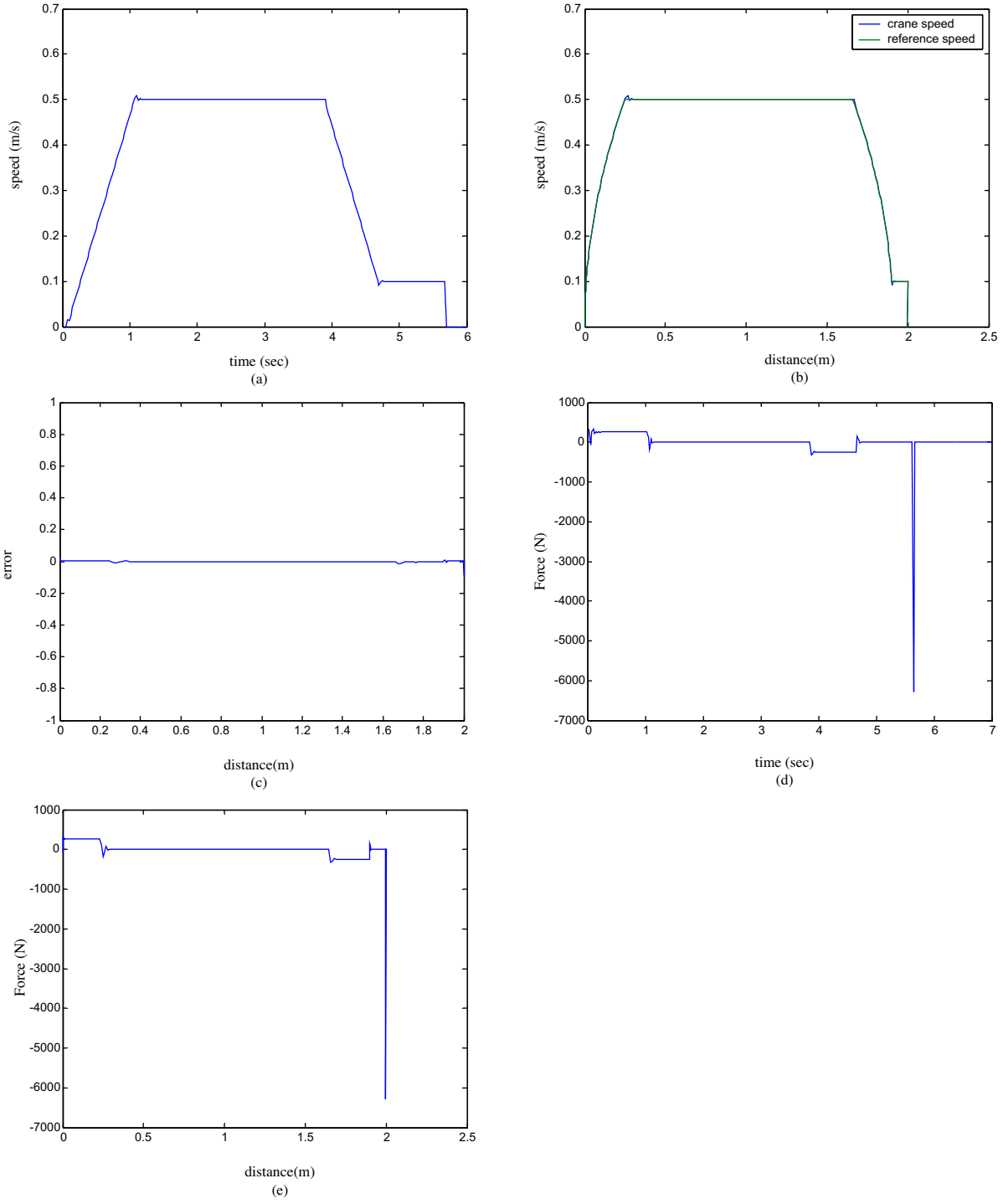

Fig. 12. *Z*-directional distance–speed control of the crane system (2 m, unloaded). (a) Time–speed curve. (b) Distance–speed curve. (c) Error between crane speed and reference. (d) Time–force curve. (e) Distance–force curve.

To achieve $\dot{V}_k \le 0$, the learning law of the compensation controller is derived as follows.

$$\dot{\tilde{c}}_{i,k} = -\dot{\hat{c}}_{i,k} = -\eta_c |s_{f,k}(t)| N_{i,j}(s_{f,k}(t)). \tag{43}$$

Therefore, (32) can be rewritten as

$$\begin{aligned}\dot{V}_k &= s_{f,k}(\varepsilon_k - \sum_{i=0}^{2p}(\hat{c}_{i,k} sgn(s_{f,k}(t)) N_{i,j}(s_k)) - \sum_{i=0}^{2p}\tilde{c}_{i,k}|s_{f,k}(t)|N_{i,j}(s_{f,k}(t))\\ &\le |s_{f,k}||\varepsilon_k| - |s_{f,k}|\sum_{i=0}^{2p}\hat{c}_{i,k}N_{i,j}(s_{f,k}) - |s_{f,k}|\sum_{i=0}^{2p}\tilde{c}_{i,k}N_{i,j}(s_{f,k})\\ &= |s_{f,k}|(|\varepsilon_k| - \sum_{i=0}^{2p}c^*_{i,k}N_{i,j}(s_{f,k})) \le 0.\end{aligned} \tag{44}$$

This implies that $\dot{V}_k$ is negative semidefinite. Define the following term

$$(45) P_k = (\sum_{i=0}^{2p}c^*_{i,k}N_{i,j}(s_{f,k}) - |\varepsilon_k|)|s_{f,k}| \le -\dot{V}_k \text{Because} \qquad V_k(0) \text{is}$$

bounded and $V_k(t)$ is nonincreasing and bounded, then

$$\int_0^t P_k(\tau)d\tau \le V_k(s_{f,k}(0), \tilde{c}_{i,k}(0)) - V_k(s_{f,k}(t), \tilde{c}_{i,k}(t)) < \infty \tag{46}$$

Also, because $\dot{P}_k(t)$ is bounded, it can be shown that $\lim_{t\to\infty} P_k(t) = 0$ by Barbalat's Lemma [21]. That is $s_{f,k} \to 0$ as $t \to \infty$, then the stability is guaranteed.

Remark: Since the auto-warehousing system works under a limited loading range, the error bound in (34) **can be given with a finite constant.** However, the chattering phenomenon of the sliding mode control is unfavorable. In this paper, with the introduction of the B-spline function, the description of the error bound is represented in a polynomial manner. In (37), the approximation of the error bound is represented based on the polynomial mapping derived from the coefficients and the B-spline basis functions. Based on the learning law of (43), only the coefficients associated with the activated basis functions are tuned. Thus, the estimation of the error bound can be represented in an effective and efficient way.

4. Simulation results

To verify the effectiveness of the proposed approach, the crane system is controlled by the ABFSM to move 10 and 30 m in the x direction, 3 and 20 m in the y direction, and 2 m in the z direction. The loading conditions for the crane system in the x, y, z directions are given in Tables 4, 5, and 6, respectively. The initial settings of the premise and consequence parameters of the AFIC are shown in Fig. 4. The parameters of the ABFSM are selected with $k_1 = 2$, $k_2 = 1, \eta_\alpha = 50, \eta_c = 10$ for the AFIC, and $p = 3, j = 2$, $\mathbf{T} = \begin{bmatrix} -20 & -2 & -0.6 & -0.2 & 0 & 0.2 & 0.6 & 2 & 20 \end{bmatrix}$, $\mathbf{C}$ is initialized with zeros and $\eta_c = 0.01$ for the BCC. The results of the 3 m motion control in the x direction with the load of 1.5×10^4kg and the 30 m motion control in the x direction without load are shown in Figs. 5 and 6, respectively. The results of the 3 m upward motion control in the y direction with the load and the 20 m upward motion control in the y direction without load are shown in Figs. 7 and 8, respectively. The results of the 3 m downward motion control in the y direction with the load of 5×10^3kg and the 20 m downward motion control in the y direction without load are shown in Figs. 9 and 10, respectively. Finally, the results of the 2 m motion control in the z direction with the load of 2×10^3kg and the 2 m motion control in the z direction without load are shown in Figs. 11 and 12, respectively.

Regarding handling disturbance and uncertainty, the performance of the traditional control techniques is acceptable if the characteristics of the controlled plant are understood at a certain level. However, with the different demands of loading and desired distance, the comprehensive understanding of the auto-warehousing crane system is difficult to achieve. The analytic modeling and the dynamic assumptions are usually inaccurate and the control gains have to be refined for specific working condition. To cope with the nonlinearity of the practical crane systems, in the proposed ABFSM, the online parameter adaptation is adopted in the fuzzy inference process. **With the introduction of the information from sliding surface as the input of the fuzzy controller, the dilemma between the controller complexity and control performance is solved when the number of fuzzy rules in the AFIC is much smaller than that in the traditional FLCs.** Thus, a simple but effective way is proposed. The results in the x, y, z direction are given in Tables 4–6, respectively, where the performance of the ABFSM are observed.

5. Conclusions

In this paper, the ABFSM has successfully applied to the motion control of the auto-warehousing system. In the AFIC, the fuzzy logic inference is introduced to provide a means to approximate the ideal controller for the crane system when its dynamics are complex to be comprehended. **To alleviate the burden of fuzzy rule construction, only the information from sliding surface is exploited as the input such that the conciseness and translucency of the control system can be upgraded.** On the other hand, the BCC aims to compensate the approximation error of the AFIC. To achieve the efficient motion control, a distance–speed reference curve for each direction is designed before the beginning of control process according to the specifications of the crane system. Thus, a powerful yet easy-to-use methodology is given for online gain determination when optimal or sup-optimal fuzzy system is difficult to obtain. Two main contributions of the paper are 1) the stability of closed-loop adaptive fuzzy controller can be guaranteed by the means of Lyapunov function, and 2) using the concept of sliding-mode control and B-spline functions, the proposed ABFSM possesses the merit of being easily undertaken by a microprocessor. To validate the performance of the proposed approach, the ABFSM is applied to the auto-warehousing crane motion control under various loading conditions for x, y, and z directions, respectively. Through the simulation results and illustrations, the feasibility and the robustness of the proposed ABFSM are verified.

References

[1] A. Balestrino, A. Landi, L. Sani, Cuk converter global control via fuzzy logic and scaling factors, IEEE Trans. Ind. Appl. 38 (2002) 406–413.
[2] J. Cao, P. Li, H. Liu, An interval fuzzy controller for vehicle active suspension systems, IEEE Trans. Intell. Transp. Syst. 11 (2010) 885–895.
[3] C.-Y. Chang, Adaptive fuzzy controller of the overhead cranes with nonlinear disturbance, IEEE Trans. Ind. Inform. 3 (2007) 164–172.
[4] C.-Y. Chen, T.-H.S. Li, Y.-C. Yeh, EP-based kinematic control and adaptive fuzzy sliding-mode dynamic control for wheeled mobile robots, Inform. Sciences 179 (2009) 180–195.
[5] K.-H. Cheng, Adaptive fuzzy CMAC-based nonlinear control with dynamic memory architecture, J. Franklin Inst. 348 (2011) 2480–2502.
[6] W.D. Chang, J.J. Yan, Adaptive robust PID controller design based on a sliding mode for uncertain chaotic systems, Chaos Soliton. Fract. 26 (2005) 167–175.
[7] H. Deng, R. Oruganti, D. Srinivasan, Neural controller for UPS inverters based on B-spline network, IEEE Trans. Ind. Electron. 55 (2008) 899–909.
[8] Y. Fang, W.E. Dixon, D.M. Dawson, E. Zergeroglu, Nonlinear coupling control laws for an underactuated overhead crane system, IEEE/ASME Trans. Mechatronics 8 (2003) 418–423.
[9] H.F. Ho, Y.K. Wong, A.B. Rad, Robust fuzzy tracking control for robotic manipulators, Simulat. Model. Pract. Theor. 15 (2007) 801–816.
[10] C.-F. Hsu, K.-H. Cheng, Recurrent fuzzy-neural approach for nonlinear control using dynamic structure learning scheme, Neurocom. 71 (2008) 3447–3459.

[11] A. Kechroud, J.J.H. Paulides, E.A. Lomonova, B-Spline Neural Network Approach to Inverse Problems in Switched Reluctance Motor Optimal Design, IEEE Trans. Magn. 47 (2011) 4179–4182.
[12] C. Li, C.-Y. Lee, Fuzzy motion control of an auto-warehousing crane system, IEEE Trans. Ind. Electron. 48 (2001) 983–994.
[13] D. Lin, X. Wang, Observer-based decentralized fuzzy neural sliding mode control for interconnected unknown chaotic systems via network structure adaptation, Fuzzy Set Syst. 161 (2010) 2066–2080.
[14] D. Lin, X. Wang, F. Nian, Y. Zhang, dynamic fuzzy neural networks modeling and adaptive backstepping tracking control of uncertain chaotic systems, Neurocom. 73 (2010) 2873–2881.
[15] D. Lin, X. Wang, chaos synchronization for a class of nonequivalent systems with restrictive inputs via time-varying sliding mode, Nonlinear Dyn. 66 (2011) 89–97.
[16] M. Lopez, L.G. Vicuna, M. Castilla, P. Gaya, O. Lopez, Current distribution control design for paralleled DC/DC converters using sliding-mode control, IEEE Trans. Ind. Electron. 51 (2004) 419–428.
[17] C.M. Lin, C.F. Hsu, Supervisory recurrent fuzzy neural network control of wing rock for slender delta wings, IEEE Trans. Fuzzy Syst. 12 (2004) 733–742.
[18] T.-H.S. Li, C.-L. Kuo, N.R. Guo, Design of an EP-based fuzzy sliding-mode control for a magnetic ball suspension system, Chaos Soliton. Fract. 33 (2007) 1523–1531.
[19] Y.-G. Leu, C.-Y. Chen, B-spline backstepping control with derivative matrix estimation and its applications, Neurocom. 74 (2011) 499–508.
[20] O. Motlagh, S.H. Tang, N. Ismail, A.R. Ramli, An expert fuzzy cognitive map for reactive navigation of mobile robots, Fuzzy Set Syst. 201 (2012) 105–121.
[21] K.S. Narendra, A.M. Annaswamy, Stable Adpative Systems, Prentice-Hall, Englewood Cliffs, NJ, 1989.
[22] Y.J. Niu, X.Y. Wang, A novel adaptive fuzzy sliding-mode controller for uncertain chaotic systems, Nonlinear Dyn. 73 (2013) 1201–1209.
[23] Y.L. Sun, M.J. Er, Hybrid Fuzzy Control of Robotics Systems, IEEE Trans. Fuzzy Syst. 12 (2004) 755–765.
[24] M. Nie, W.W. Tan, Stable adaptive fuzzy PD plus PI controller for nonlinear uncertain systems, Fuzzy Set Syst. 179 (2011) 1–19.
[25] Y.Y. Tzou, S.Y. Lin, Fuzzy-tuning current-vector control of a three phase PWM inverter for high-performance AC drive, IEEE Trans. Ind. Electron. 45 (1998) 782–791.
[26] D.L. Tsay, H.Y. Chung, C.J. Lee, The adaptive control of nonlinear systems using the sugeno-type of fuzzy logic, IEEE Trans. Fuzzy Syst. 7 (1999) 225–229.
[27] S. Tong, Y. Li, Observer-based fuzzy adaptive control for strict-feedback nonlinear systems, Fuzzy Set Syst. 160 (2009) 1749–1764.
[28] C.C. Wong, J.Y. Chen, Fuzzy control of nonlinear systems using rule adjustment, IEE Proc. Control Theory Appl. 146 (1999) 578–584.
[29] W.Y. Wang, M.L. Chen, C.C.J. Hsu, T.T. Lee, tracking-based sliding mode control for uncertain nonlinear systems via an adaptive fuzzy-neural approach, IEEE Trans. Syst. Man Cybern. B Cybern. 32 (2002) 483–492.
[30] R.J. Wai, C.M. Lin, C.F. Hsu, Adaptive fuzzy sliding-mode control for electrical servo drive, Fuzzy Set Syst. 143 (2004) 295–310.
[31] X. Wang, X. Zhang, C. Ma, Modified projective synchronization of fractional-order chaotic systems via active sliding mode control, Nonlinear Dyn. 69 (2012) 511–517.
[32] B. Yoo, W. Ham, Adaptive fuzzy sliding mode control of nonlinear system, IEEE Trans Fuzzy Syst. 6 (1998) 315–321.
[33] Z. Yu, Z. Man, B. Wu, Design of fuzzy sliding-mode control systems, Fuzzy Set Syst. 95 (1998) 295–306.
[34] S. Yu, X. Yu, Z. Man, A fuzzy neural network approximator with fast terminal sliding mode and its applications, Fuzzy Set Syst. 148 (2004) 469–486.
[35] X. Yu, O. Kaynak, Sliding-mode control with soft computing: A survey, IEEE Trans. Ind. Electron. 56 (2009) 3275–3285.